

## University of Dayton eCommons

Electrical and Computer Engineering Faculty  
Publications

Department of Electrical and Computer  
Engineering

8-1995

# Broadband Dynamic, Holographically Self-Recorded, and Static Hexagonal Scattering Patterns in Photorefractive KNbO<sub>3</sub>:Fe

Nickolai Kukhtarev  
*Alabama A & M University*

Tatiana V. Kukhtareva  
*Alabama A & M University*

John Caulfield  
*Alabama A & M University*

Partha P. Banerjee  
*University of Dayton, pbanerjee1@udayton.edu*

Hsueh-Ling Yu  
*University of Alabama, Huntsville*

*See next page for additional authors*

Follow this and additional works at: [https://ecommons.udayton.edu/ece\\_fac\\_pub](https://ecommons.udayton.edu/ece_fac_pub)

 Part of the [Computer Engineering Commons](#), [Electrical and Electronics Commons](#), [Electromagnetics and Photonics Commons](#), [Optics Commons](#), [Other Electrical and Computer Engineering Commons](#), and the [Systems and Communications Commons](#)

### eCommons Citation

Kukhtarev, Nickolai; Kukhtareva, Tatiana V.; Caulfield, John; Banerjee, Partha P.; Yu, Hsueh-Ling; and Hesselink, Lambertus, "Broadband Dynamic, Holographically Self-Recorded, and Static Hexagonal Scattering Patterns in Photorefractive KNbO<sub>3</sub>:Fe" (1995). *Electrical and Computer Engineering Faculty Publications*. 178.  
[https://ecommons.udayton.edu/ece\\_fac\\_pub/178](https://ecommons.udayton.edu/ece_fac_pub/178)

This Article is brought to you for free and open access by the Department of Electrical and Computer Engineering at eCommons. It has been accepted for inclusion in Electrical and Computer Engineering Faculty Publications by an authorized administrator of eCommons. For more information, please contact [frice1@udayton.edu](mailto:frice1@udayton.edu), [mschlangen1@udayton.edu](mailto:mschlangen1@udayton.edu).

---

**Author(s)**

Nickolai Kukhtarev, Tatiana V. Kukhtareva, John Caulfield, Partha P. Banerjee, Hsueh-Ling Yu, and Lambertus Hesselink

# Broadband dynamic, holographically self-recorded, and static hexagonal scattering patterns in photorefractive $\text{KNbO}_3\text{:Fe}$

Nickolai V. Kukhtarev, MEMBER SPIE

T. Kukhtareva

H. John Caulfield, FELLOW SPIE

Alabama A&M University

Center for Applied Optical Sciences

Department of Physics

Normal, Alabama 35762

Partha P. Banerjee

Hsueh-Ling Yu

University of Alabama in Huntsville

Department of Electrical and Computer

Engineering

Huntsville, Alabama 35899

Lambertus Hesselink

Stanford University

Department of Electrical Engineering

Stanford, California 94305

**Abstract.** We have observed and explained three types of hexagon pattern formation in photorefractive crystal  $\text{KNbO}_3\text{:Fe}$ . These are: (1) dynamic (laser induced), (2) semipermanent (holographically stored), (3) permanent (induced by a static domain grid) over a wide wavelength range.

*Subject terms:* photorefractive nonlinear optics; hexagonal scattering pattern; nonlinear self-organization of scattering; photorefractive materials.

*Optical Engineering* 34(8), 2261–2265 (August 1995).

## 1 Introduction

Under far from equilibrium conditions, highly structured, self-organized phenomena often occur—usually with some threshold of the driving or pumping power. Because hexagonal packing is ultracompact and ultrastable, it is not unreasonable to find such a state as an attractor once the rearrangement energy is provided. Thus soap bubbles, beehives, compound eyes, fiber optic bundles, and many other structures exhibit that symmetry.<sup>1–3</sup>

A laser beam incident on a nonlinear material may offer a way to observe such self-organizing structures. The beam serves two purposes simultaneously: pump and probe. If the material arranges itself in a hexagonal fashion, we expect the scattered light to form a hexagonal spot array (HSA). This phenomenon has been observed in gases,<sup>4,5</sup> liquid crystals,<sup>6,7</sup> and the photorefractive crystal<sup>8,9</sup>  $\text{KNbO}_3$ . The self-organized hexagonal structure appears to be a universal attractor in such situations.

Our work<sup>9</sup> on  $\text{KNbO}_3$  has shown not only direct images of the hexagonal inhomogeneities in the crystal and the resulting HSA but also that rotation of those patterns can be effected by laser-beam irradiance.

This paper is a continuation of our prior work on HSA formation and reconfiguration through rotation of the pattern.<sup>9</sup> Here, we report observation of reconfigurable HSAs in the different colors, ranging from blue-green from an Ar

laser to red from a low-power HeNe laser ( $P < 20$  mW) in  $\text{KNbO}_3$ . We also show that nonlinear dynamic HSA can be holographically self-recorded in the same crystal and retrieved with a reference beam. In addition, we have observed static (linear) hexagonal scattering due to 60-deg domain structures in  $\text{KNbO}_3$ . These observations imply that a photorefractive crystal (such as  $\text{KNbO}_3$ ) may give us a complete set of hexagonal patterns: dynamic (with possibility of recording), semipermanent, and static in different colors, including low-power HeNe red light.

## 2 Experimental Results

Holographic self-recording offers a new possibility for the investigation of different stages of the complex self-organization dynamics in a photorefractive crystal. Our simple experimental setup (see Fig. 1) comprises only a few elements: a laser (He-Ne or Ar), a lens of focal length 70 cm, two beamsplitters (BS1, BS2), and the photorefractive crystal. The scheme in Fig. 1 allows us to do hexagon generation and holographic recording simultaneously.

In the experiment the horizontally polarized signal beam  $E_F$  is normally incident on the crystal surface, allowing overlapping with reflected beam  $E_B$  from the real crystal surface. The far-field pattern, with no  $E_1$ , is stationary in time and comprises a strong central spot with a peripheral ring, which appears “instantaneously” and thereafter evolves into six symmetrically spaced spots. This far-field pattern is observed simultaneously in both the forward and backward directions; however, the diffraction efficiencies (discussed in more detail below), are not identical.

Paper PN-006 received Jan. 20, 1995; revised manuscript received April 18, 1995; accepted for publication April 26, 1995.

© 1995 Society of Photo-Optical Instrumentation Engineers. 0091-3286/95/\$6.00.

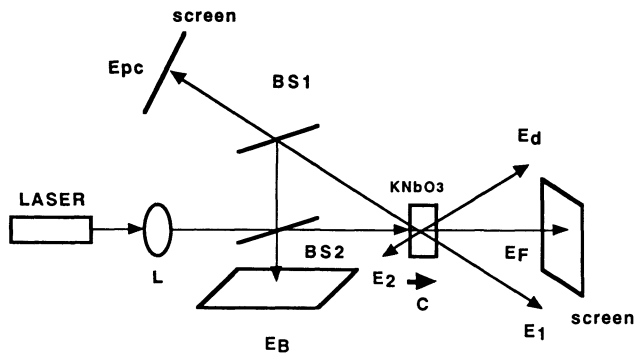


**Fig. 1** Scheme of hexagon pattern generation and holographical self-recording.

The semiangle of divergence  $\nu$  of the peripheral cone is approximately 0.8 deg for an operating wavelength of 514 nm (from the Ar laser), and is independent of the incident power. The time taken to form the spots is a few seconds for an incident power of 7.5 mW, space focused into a 0.5-mm-diam beam. The ring and all spots (central and peripheral) are also predominantly horizontally polarized. The diffraction efficiency for the spots in the forward direction is large: the intensity ratio of each transmitted peripheral spot to the transmitted central spot, which we term the diffraction efficiency per spot, is over 7%. The corresponding diffraction efficiency in the backward direction is about 4% per spot. We believe that a contributing reason for this is the reflection of part of the input beam from the incident interface. The experiment was repeated at wavelengths of 632 nm (from the He-Ne laser) and  $\lambda = 440$  nm (from the Ar laser). In all cases, HSA formation is observed. For instance, at 632 nm,  $\nu = 1$  deg and the minimum power needed is 20 mW for a beam diameter  $\approx 3$  mm.

If the incident beam is slightly off normal to the interface (typically by 0.04 deg) and the power is increased, the entire hexagonal pattern rotates. The sense of rotation depends on the angular misalignment. Thus, both clockwise and counterclockwise rotations of the pattern are possible through positive and negative angular misalignments. A typical value for the rotation speed in the steady state is 100 deg/min for an incident power of 30 mW in the 0.08-cm<sup>2</sup> spot at an operating wavelength of 514 nm. Details of other experimental observations, effects of higher power, larger misalignment, etc., at 514 nm may be found in Ref. 9.

In the second stage of the experiment, we have studied the recording and readout properties of the hologram responsible for HSA formation. To this end, a second beam, which we call reference beam  $E_1$ , is incident at a small angle  $\nu \approx 5$  to 10 deg, which is larger than the cone angle of induced hexagon scattering ( $\varphi_h = 0.8$  deg). After exposure for about 1 min, cone scattering, which thereafter rearranges into a hexagon, appears in both transmitted ( $E_F$ ) and reflected ( $E_B$ ) beams, together with additional beams in the forward ( $E_d$ ) and backward ( $E_{pc}$ ) directions ( $E_{pc}$  is counterpropagating to  $E_1$ ) are observed.

After blocking  $E_F$  with a shutter, the holographic image of a hexagon slowly decays after over about a minute, along with decaying signals  $E_{pc}$  and  $E_d$  (Fig. 2).

While both the above experiments show the presence of nonlinearly induced HSAs, characterized by a threshold, we

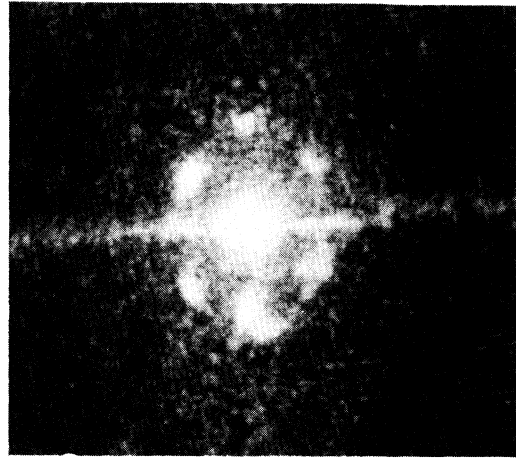


**Fig. 2** Holographic image of a hexagon in KNbO<sub>3</sub> made with HeNe.

have also observed linear scattering into HSAs at all powers and wavelengths specified above, albeit with a much larger scattering angle. For instance, for  $\lambda = 632$  nm, the linear scattering angle is approximately 9 deg.

### 3 Theory

#### 3.1 Hexagon Formation and Rotation

For pattern formation we propose a holographic model with transmission gratings, formed by initial forward and scattered waves, which overlap with similar gratings, created from backward reflected and scattered waves, due to local nonlinearities. Reflection gratings, formed by the input beam and its reflection from the rear crystal face, may change the effective reflection coefficient and can influence the threshold condition for instabilities. It can be shown that in steady state, the "dispersion" relation for transversal instability with wave number  $K$  may be expressed as

$$\left(\frac{1}{R} + R\right) + 2 \cos k_d L \cosh \Gamma L + \left\{ \frac{k_d}{\Gamma} - \frac{\Gamma}{k_a} + \frac{2g}{\Gamma \gamma^2 R} (2\gamma^2 \sqrt{R} - \gamma g) - 2\gamma^2 R \sqrt{R} + \gamma R g \right\} \sinh \Gamma L \sin k_d L + \frac{2g}{k_d \gamma R} (g - 2\gamma \sqrt{R}) \sin^2 k_d L - \frac{g}{\gamma^2 R} \left\{ g - 2\gamma \sqrt{R} - \frac{k_d}{\Gamma^2} (2k_d \gamma \sqrt{R} - 4\gamma^2 \sqrt{R} - k_d g + 2\gamma g) \right\} \sinh^2 \Gamma L = 0, \quad (1a)$$

with

$$\Gamma^2 = 2k_d\gamma(1+R) - k_d^2, \quad \gamma = -\frac{k_0\gamma_T}{1+L_{DT}^2K^2}A^2,$$

$$g = k_0\gamma_R A^2 \sqrt{R}, \quad k_d = \frac{K^2}{2k_0 n_o}. \quad (1b)$$

In (1),  $\gamma_{T,R}$  are nonlinearity coefficients associated with transmission and reflection gratings,  $L_{DT}$  is a characteristic diffusion length associated with the transmission grating,  $R$  is the reflection coefficient at the interface,  $k_0$  is the wave number of the light in free space,  $n_o$  is the pertinent refractive index, and  $A$  is the amplitude of the incident beam. In the above relation, the contribution from reflection gratings has been assumed to be small. Details of the derivation will be presented elsewhere; suffice it to state that the result is an extension of the work in Refs. 10, 11 that treats transmission and reflection gratings separately. We assume a self-defocusing nonlinearity, which is evident from experimental results of a  $z$ -scan at 514 nm in the forward direction.<sup>9</sup> Figure 3 shows the dispersion curves for various values of  $gL$ . Note that, as anticipated earlier, the threshold for the onset of instabilities decreases with increasing  $|gL|$ , making the onset of instabilities more practically realizable. Note also that there is a small change in the corresponding  $K$  (which determines the cone angle) for the lowest threshold (as depicted by the minimum points on the set of curves) with increasing  $|gL|$ .

To further reconcile the result of (1) with previous results<sup>9</sup> for  $g = 0$ , the dispersion relation may be reduced to the form

$$\frac{1+R^2}{R} = -2 \cos k_d L \cosh \Gamma L - \left( \frac{k_d}{\Gamma} - \frac{\Gamma}{k_d} \right) \sin k_d L \sinh \Gamma L. \quad (2)$$

From Fig. 3, the minimum of the curve is around  $k_d L = \pi$ , which is in agreement with earlier results on the cone angle. Also, with this substitution in Eq. (2), the relation reduces to

$$k_0\gamma_T A^2 L \approx \frac{1}{\sqrt{R}}, \quad (3)$$

which shows that the threshold decreases with increasing  $R$ .

The above threshold calculation only shows that if the incident intensity is above the value in Eq. (1), a single beam may nonlinearly induce the formation of a ring, which is the first stage of the self-organization process. The transition to HSA from the ring has been discussed in detail in Refs. 9,12,13.

One peculiar feature of our experiment is a constant-speed rotation of the hexagonal pattern in the far field through a small misalignment (about 0.04 deg) from its nominally normal incidence.<sup>9</sup> The speed of rotation is proportional to the laser intensity and is of the order of 0.05 rad (or 2.85 deg) per second. The sense of rotation can be reversed by reversing the sign of the tilt angle.

Our proposed two-stage holographic model of pattern formation can also explain the rotation of the hexagonal pattern

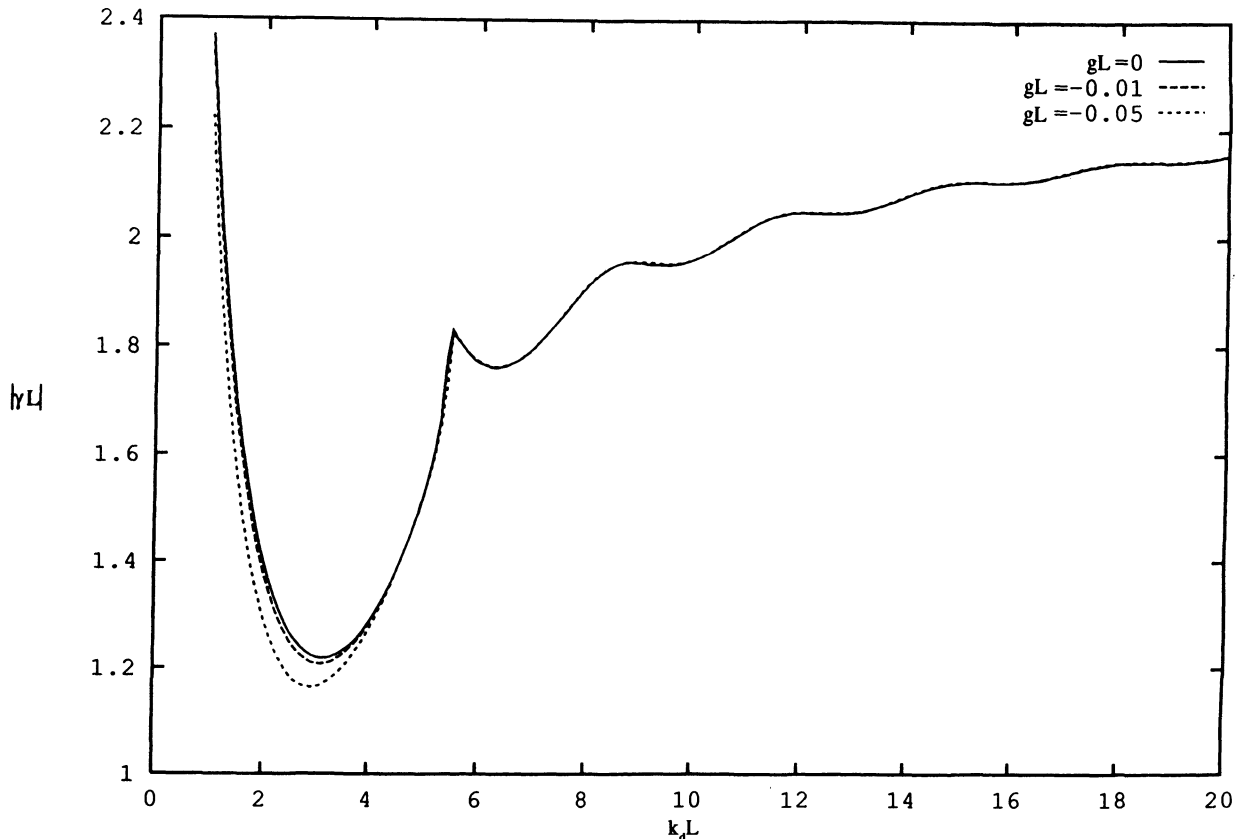


Fig. 3 Dispersion relation,  $R=0.4$ , showing dependence of threshold on contribution from the reflection gratings.

by dynamic phase transfer between interacting waves. In the first stage, scattering waves originating from forward- and backward-reflected waves rearrange in a cone while forming an array of gratings. The apex angle  $\nu$  of the cone (approximately 1 deg) is determined by phase-matching conditions when geometrical mismatch is compensated by the nonlinear change in the grating wave vector. In the second stage, waves whose wave vectors end on the cone begin to write gratings between themselves. For a cubic nonlinearity, this naturally leads to a hexagon-type rearrangement of the cone scattering. Master gratings, formed by the central and peripheral beams, are running gratings due to phase transfer between waves with unequal intensities. For the symmetric case of normal incidence, the movements of different gratings get balanced and a stable far-field hexagonal pattern can be observed, stabilized by a slight anisotropy due to the photorefractive grating.

However, when a small deviation angle  $\theta$  is introduced, the movement of different gratings cannot be balanced, and a phase difference between adjacent hexagonal spots appears. This phase difference leads to rotation of the pattern with the angular velocity  $\Omega = (d \Delta n / dt) (I_p / I_0) \theta$ , where  $d \Delta n / dt = \alpha I_0$  is the time rate of change of the nonlinearity induced index change,  $I_{p,0}$  are the intensities of the peripheral and central spots, and  $\alpha$  is a nonlinear coupling coefficient. The rate of rotation is linear in the intensity of the incident beam, and the change in sign of  $\theta$  is in agreement with our experimental results.

### 3.2 Hologram Recording and Readout

For an explanation of the appearance of new beams  $E_d$  and  $E_{pc}$  as stated in Sec. 2 and of the hexagon holographic recording, we introduce a six-wave mixing model, by analogy with self-phase-conjugation geometry, realized in SBN.<sup>14</sup>

The scattering diagrams show directions of the diffracted wave vectors (Fig. 4, left side) as a sum of contributions (right side) due to scattering of waves (dashed arrows) on the recorded gratings (solid arrows). These scattering diagrams help us to write down the following coupled wave equations for  $E_d$  and  $E_{pc}$ :

$$\frac{dE_d}{dz} = \gamma_{B2} \langle E_B E_2^* \rangle E_F + \gamma_{F2} \langle E_F E_2^* \rangle E_B ,$$

$$\frac{dE_{pc}}{dz} = \gamma_{F1} \langle E_F E_1^* \rangle E_B + \gamma_{B1} \langle E_B E_1^* \rangle E_F , \quad (4)$$

where  $\gamma_{B2}, \gamma_{F2}, \gamma_{F1}, \gamma_{B1}$  are coupling constants, and  $\langle \cdot \rangle$  means time integration over the relaxation time  $\tau$ . From Eq. (4) one can see that for plane waves  $E_1$  and  $E_2$  in the steady state,  $E_d \approx E_F E_B$ , which means that the diffracted intensity is the product of pump wave intensities, while the phase is the sum of the phases of the forward and backward waves. ("Convolution" may be a good term for describing this optical operation in the language of optical processing.)

It is easy to show that on blocking the  $E_F$  wave, diffraction of  $E_1$  will lead to a wave  $E_d$  (for time  $t \geq t_B$ ) given by

$$E_d = \gamma_{F1} \langle E_F E_1^* \rangle_{t=t_B} \exp\left(\frac{t_B - t}{\tau}\right) E_1 , \quad (5)$$

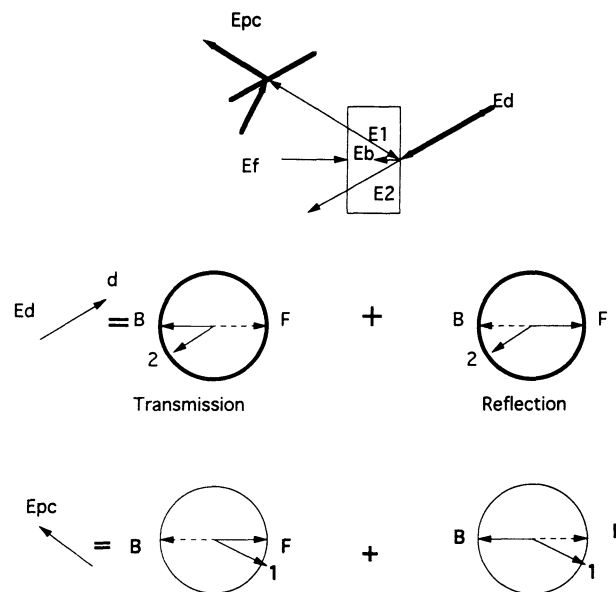


Fig. 4 Scattering diagrams of six-wave mixing, describing formation of diffracted ( $E_d$ ) and phase-conjugated waves ( $E_{pc}$ ) by transmission and reflection gratings.

which is a holographic copy of the  $E_F$  wave (in our case, the "hexagon" wave) decaying with a time constant  $\tau$ .

### 3.3 Linear HSA Formation

The linear hexagon-type scattering, which is marked by the absence of any threshold intensity, can be explained by scattering from 60-deg domain-wall structures in doped crystals<sup>15</sup> in which impurities act as nucleation centers for domain formation. Direct observation of the crystal  $C$  face in a polarized microscope supports this explanation (see Fig. 5).

In passing, we would like to note that the correlation in shape between nonlinear and linear HSA formation may be attributed to 60-deg domain walls nucleated around photo-sensitive impurities in the former case.

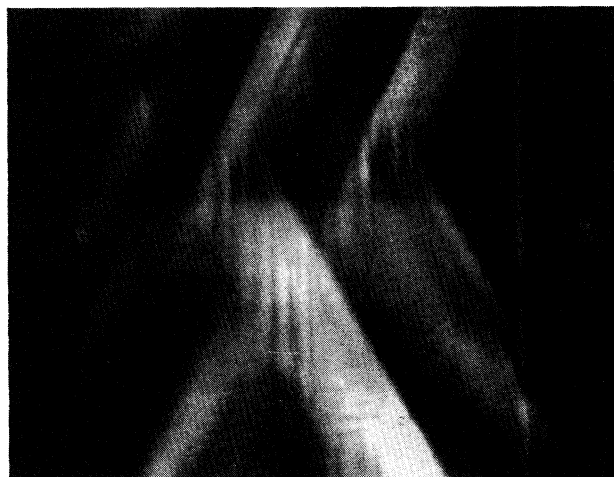


Fig. 5 Picture of 60-deg domain walls as seen in a polarized microscope on the  $C$  face of  $\text{KNbO}_3$  ( $M=625$ ).

## 4 Conclusion

To summarize, we have shown the natural nonlinear reorganization of light into a stable hexagonal spot array over a broad range of frequencies. The HSA may indeed be perceived as a basin of attraction of the nonlinear dynamical system comprising the interaction of a primary wave and scattered waves. We have also demonstrated that a dynamic HSA can be holographically self-recorded in the crystal and read out by a reference beam. Finally, we have shown the presence of linear HSAs and suggested that the occurrence of nonlinear HSAs may be due to mechanisms similar to that responsible for linear scattering, at a microscopic level.

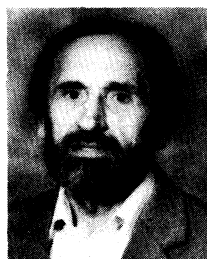
## Acknowledgments

The AAMU work is partially supported by USAF Office of Scientific Research (AFOSR) contract No. F49620-93-1-0123 and by NSF grant 8802971. The work at Stanford University was partially supported by ARPA under the URI program and by the Center for Nonlinear Optical Materials (CNOM).

## References

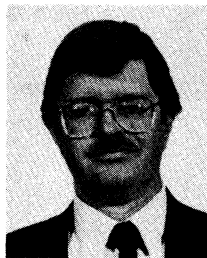
1. R. M. Mersereau, "The processing of hexagonally-sampled 2d-dimensional signals," *Proc. IEEE* **67**, 930 (1979).
2. V. Killat, G. Rabe, and W. Rave, *Fiber and Integrated Opt.* **4**, 159 (1980).
3. A. B. Watson and A. J. Ahumada, "A hexagonal orthogonal oriented pyramid as a model of image representation in visual cortex," *IEEE Trans. Biomed. Eng.* **36**, 97 (1989).
4. J. Pender and L. Hesselink, "Degenerate conical emission in atomic-sodium vapor," *J. Opt. Soc. Am. B* **7**, 1361 (1990).
5. A. Grynberg, E. LeBihan, P. Verkerk, P. Simoneau, J. R. R. Leite, D. Bloch, Le Boiteaux, and M. Ducloy, "Observation of instabilities due to mirrorless four-wave mixing oscillation in sodium," *Opt. Commun.* **67**, 363 (1988).
6. B. Thuring, R. Neubecker, and T. Tschudi, "Transverse pattern formation in liquid crystal light valve feedback system," *Opt. Commun.* **102**, 111 (1993).
7. R. Macdonald and H. J. Eichler, "Spontaneous optical pattern formation in a nematic liquid crystal with feedback mirror," *Opt. Commun.* **89**, 289 (1992).
8. T. Honda, "Hexagonal pattern formation due to counterpropagation in  $\text{KNbO}_3$ ," *Opt. Lett.* **18**, 598 (1993).
9. P. P. Banerjee, H. Yu, D. A. Gregory, N. Kukhtarev, and H. J. Caulfield, "Selforganization of scattering in photorefractive  $\text{KNbO}_3$  into a reconfigurable hexagonal spot array," *Opt. Lett.* **20**, 10 (1995).
10. M. Saffman, D. Montgomery, A. A. Zozulya, K. Kuroda, and D. Z. Anderson, "Transverse instability of counterpropagating waves in photorefractive media," *Phys. Rev. A* **48**, 3209 (1993).
11. M. Saffman, A. A. Zozulya, and D. Z. Anderson, "Transverse instability of energy-exchanging counterpropagating waves in photorefractive media," *J. Opt. Soc. Am. B* **11**, 1409 (1994).
12. G. D' Alessandro and W. Firth, "Hexagonal spatial patterns for a Kerr slice with a feedback mirror," *Phys. Rev. A* **46**, 537 (1992).
13. S. Akhmanov, M. Vorontsov, M. Ivanov, V. Larichev, and M. Zheleznych, "Controlling transverse-wave interactions in nonlinear optics: generation and interaction of spatiotemporal structures," *J. Opt. Soc. Am. B* **9**, 78 (1992).

14. N. Bogodaev, Y. Kuz'minov, N. Kukhtarev, and N. Polozkov, "Photoinduced adaptive mirror and optical generation in photorefractive barium-strontium niobate crystals," *Sov. Tech. Phys. Lett.* **12**, 608 (1987).
15. S. G. Ingle and K. S. Moon, "Domain formation by impurity dipoles in  $\text{KNbO}_3$  single crystals," *J. Phys. D* **24**, 1637 (1991).



**Nickolai V. Kukhtarev** received his PhD in semiconductor physics in 1973 and the degree of Doctor of Physical and Mathematical Sciences in 1983 from the Institute of Physics, Kiev, Ukraine. He has been specializing in nonlinear optics and solid-state physics, and his major field of study has been dynamic holography and photorefractive physics, where he is considered to be among the founders. He is a coauthor of the world's first book on dynamic holography (1983, in Russian) and has had more than 100 papers published in refereed journals. He has been honored as a visiting scientist at Stanford University, the University of Southern California, the University of Arizona, and the University of Arkansas (USA), and at the Technical University of Berlin and the University of Osnabruck (Germany). Since 1992 he has been a research professor at Alabama A&M University, Normal (USA) and an Adjunct Senior Scientist at the Institute of Physics, Kiev, Ukraine.

**T. Kukhtareva:** biography and photograph not available.



**H. John Caulfield** received his BS from Rice University in 1958 and his PhD from Iowa State University in 1962. He was director of the Center for Applied Optics, University of Alabama at Huntsville, from 1985 to 1991, and is currently an Eminent Scholar at Alabama A&M. He was the editor of *Optical Engineering* from 1975 to 1985. He is a fellow of the Optical Society of America, a fellow of SPIE, and a senior member of IEEE.

**Partha P. Banerjee:** Biography and photograph appear with the special section guest editorial in this issue.



**Hsueh-Ling Yu** received her BS degree in nuclear engineering at the National Tsing-Hua University and her MS degree in optical engineering at the National Central University in Taiwan. She worked at the Institute of Industrial Technology in Taiwan after she received her MS degree. Yu is currently a PhD student and working with Dr. Banerjee at the University of Alabama in Huntsville. Her research interest is in nonlinear photorefractive materials.

**Lambertus Hesselink:** biography and photograph not available.